Heterogenous firing responses leads to diverse coupling to presynaptic activity in a simplified morphological model of layer V pyramidal neurons

Y. Zerlaut[1,2] & A. Destexhe[1,2]

February 3, 2016

I Abstract

Growing experimental evidences suggest that cortical processing of sensory input relies on the differential activation of neurons within cortical networks, the circuit or cellular mechanisms underlying this . In a companion communication (Zerlaut et al., 2016), we reported how individual neurons differ in their excitability and sensitivities to the properties of the membrane potential fluctuations. In the present report, we investigate how this heterogeneity is translated into diverse input-ouput properties (i.e. in th relation from presynaptic quantities to spiking probability).

To this purpose, we designed a simplified morphological model of layer V pyramidal neurons with a dendritic tree following Rall's branching rule. We first show that we are able to calibrate this simplified model on *in vitro* measurements of somatic input impedance in layer V pyramidal neurons of juvenile mive visual cortex. We then propose and analytical derivation for the membrane potential fluctuations at the soma as a function of the properties of the synaptic bombardment.

We study the coupling to different form of presynaptic activities, either balanced, unbalanced, proximal, distal, etc..

II Introduction

[. . .]

Experimental evidence accumulate to show how the diverse activation of neurons within a neocortical population might be the substrate of

Though this diverse activation is likely to be due to specific connectivity schemes, we explore here a complementary mechanism: given the strong heterogeneity in electrophysiological properties of neocortical pyramidal cells

[1] Unité de Neurosciences, Information et Complexité, Centre National de la Recherche Scientifique, FRE 3693, Gif sur Yvette, France

[2] European Institute fo Theoretical Neuroscience, 74 Rue du Faubourg Saint-Antoine, 75012 Paris

correspondance : <lastname>@unic.cnrs-gif.fr

III Results

III.1 A theoretical framework for single cell computation

taken from previous paper, to be adapted

Determining the cellular input-output functions is complex because input of neocortical neurons are mostly in dendrites and output spikes are generated in initial segments of an axon as reviewed in Stuart and Spruston (2015) and Debanne et al. (2011) input will therefore crucially shape their input-output relationship. Various parameters of presynaptic activity can arbitrarily control the properties of the membrane potential fluctuations at the soma. Those properties can be quantified by identifying three somatic variables that provide a reduced description of the dynamical state at the soma in the *fluctuation-driven* regime: the mean μ_V, the standard deviation σ_V of the membrane potential fluctuations and their typical autocorrelation time τ_V (see Methods*sec:autocorrel-def*). For example, the excitatory/inhibitory balance controls the mean depolarization at the soma μ_V, the mean synaptic bombardment impacts the standard deviation σ_V and the speed of the membrane potential fluctuations τ_V. Other effects such as synchrony in the presynaptic spike trains or ratio between distally and proximally targeting synaptic activity also affect the statistical properties of the fluctuations. The effects of synaptic input and its dendritic integration on somatic variables can be investigated theoretically using cable theory (Tuckwell et al., 2002) and will be the focus of a future communication.

Because the spike initiation site lies electrotonically close to the soma (Debanne et al., 2011), we assume that those three purely somatic variables will define the firing rate uniquely. In this study we investigate the firing response in terms of those somatic variables (illustrated in Figure *fig:3D-motiv*).

III.2 A simplified morphological model of layer V pyramidal neurons

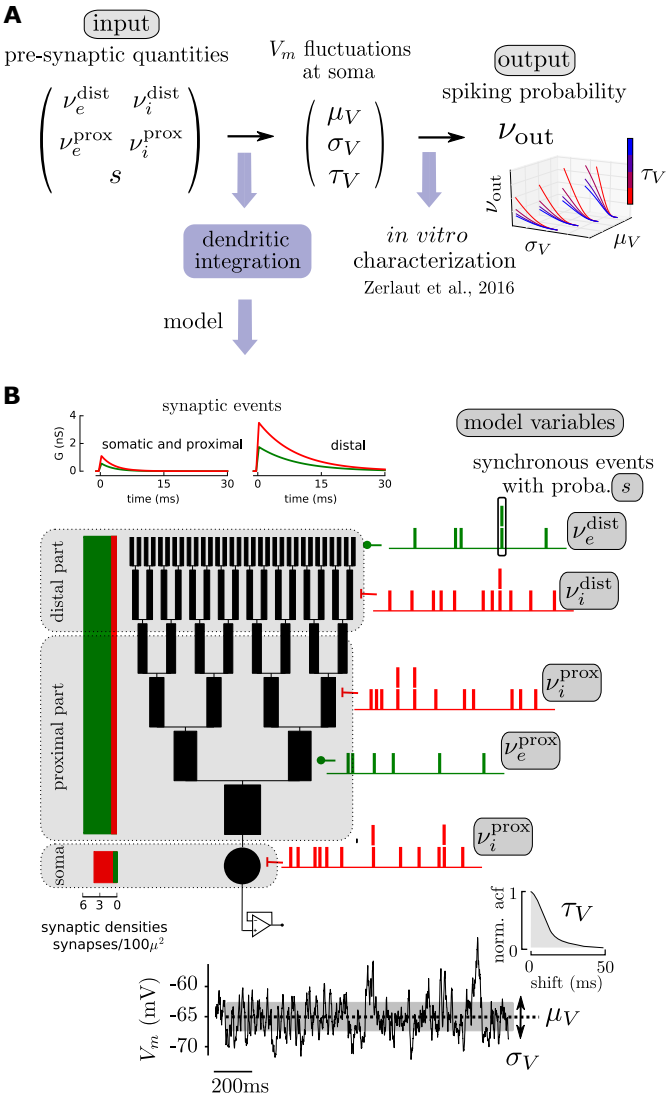

Figure 1: A theoretical framework for single cell computation in the fluctuation-driven regime. (A) Theoretical paradigm: to get the input-output function of a single cell, we split the relation from presynaptic quantities (the input) to the spiking probability (the output) into two steps. 1) passive dendritic integration shape the membrane potential at the soma and 2) how those fluctuations are translated into spikes is captured by a firing response function determined *in vitro* (Zerlaut et al., 2016) **(B)** Theoretical model for dendritic integration. A single cell is made of a lumped impedance somatic compartment and a dendritic tree. The dendritic tree is composed of B branches (here B=5), the branching is symmetric and follow Rall's 3/2 rule for the branch diameters. Synapses are then spread all over the membrane according to physiological synaptic densities. We define 3 domains: a somatic and proximal domain as well as a distal domain, excitatory and inhibitory synaptic input can vary independently in those domains. An additional variable: synaptic synchrony controls the degree of coincidents synaptic inputs.

III.3 Calibrating the morphological model on *in vitro* measurements

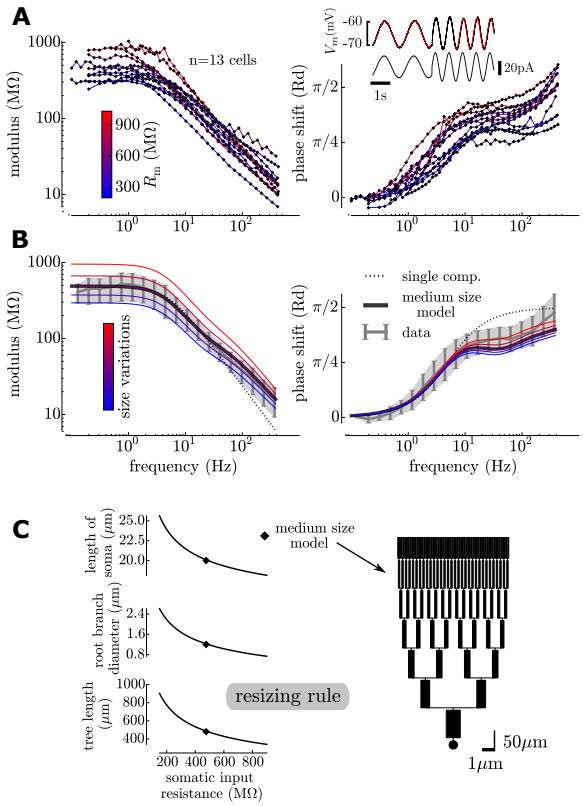

Figure 2: Calibrating the model on *in vitro* measurements: the simplified model and its size variations provides an approximation for the somatic input impedance and its heterogeneity. **(A)** Input impedance (left: modulus and right: phase shift) measured at the soma in intracellular recordings with sine-wave protocols in current-clamp (inset). The color code indicates the input resistance and is likely to result from size variations of individual cells. **(B)** A medium size model accounts for the average data and varying the size of the dendritic tree and soma reproduces the trend in the individual measurements. Large cells (blue) have a lower modulus and a lower phase shift while small cells (red) have both a higher modulus and phase shift. **(C)** Left: We obtain a map between input resistance and size of the morphological model. Right: Representation of the medium-size model.

III.4 An analytical approximation for the properties of the membrane potential fluctuations

Needed because simulations of morphologies are computationally very expensive, very limited scan of input space is allowed.

comparison between analytical approx and simulations in `NEURON`

We emphasize here that even if the analytical description uses the reduction to the equivalent cylinder (and therefore could be seen as equivalent to the Ball and Stick model), the described model has separate branches so that the fluctuations are uncorrelated from branches to branches unlike in the Ball and Stick model.

```
./to_be_done.pdf
```

Figure 3: Accuracy of the analytical approximation for the properties of the membrane potential fluctuations: comparison between numerical simulations and analytical estimates.

III.5 diverse coupling

IV Discussion

IV.1 An analytical model for dendritic integration in the fluctuation-driven regime

we provided a stratey for the analytical treatment of dendritic integration in the fluctuation-driven regime that relies on 1) shotnoise theory, 2) cable theory and 3) adequate approximations.

The main advantage of this model is that you can very naturall plug in physiological parameters (because surface area is physiological as well as transfer resistance to soma) and still it remains analytical.

Literature suffers from the reduction to single-compartment

The current model provides a tool to make network dynamics question amenable to mathematical analysis with morphologically detailed models.

IV.2 Heterogeneity of morpological and passive neuronal properties

In this study, the rescaling rule between input resistance at the soma and the morphological model has led to a relative

Table 1: Model parameters

Parameter Name	Symbol	Value	Unit
leak resistance density	r_m		

IV.3 Diverse coupling to presynaptic activity

V Material and Methods

V.1 Neuronal model

The model is illustrated on Figure 1B.

- morphology with symmetric branching
- different properties for the proximal part vs the distal part

V.2 Compartementalization

proximal vs. distal

various synaptic properties to obtain the location independence at the soma (**?**).

V.3 Correlation generator

Very simplistic model, synchrony is not shared across synapses. We duplicate spikes of one synapse with probability s.

V.4 Model equations: synaptic input and passive properties

The cable equation describes the temporal evolution and spatial spread of the membrane potential along the branches of the dendritic tree (**?**):

$$\frac{1}{r_i}\frac{\partial^2 v}{\partial x^2} = i_m(v,x,t) = c_m\frac{\partial v}{\partial t} + \frac{v-E_L}{r_m} - i_{syn}(v,x,t) \quad (1)$$

the membrane current $i_m(v,x,t)$ is a linear density of current (the presented cable equation already includes the radial symmetry). Though the modeled system has several branches, the equation can be written as a single spatial dependency x because the symmetry of the model across branches imply that the properties of the input are identical at a given distance to the soma.

Synaptic input is modeled by local (infinitely small) and transient changes of membrane permeability to selective ionic channels. Both excitatory (accounting for AMPA synapses) and inhibitory synapses (accounting for GABAa synapses) are considered, their reversal potential is E_e=0mV and E_i=-80mV respectively. Each synaptic event is generated by a shotnoise and its effect on the conductance is a jump followed by an exponential decay. The form of the synaptic current is therefore:

$$\begin{cases} i_{syn}(v,x,t) = g_e(x,t)(E_e - v) + g_i(x,t)(E_i - v) \\ g_e(x,t) = \sum_{\{x_e,\{t_e\}\}} \delta(x-x_e)\sum_{t_e}\mathcal{H}(t-t_e)Q_e(x)\,e^{-\frac{t-t_e}{\tau_e(x)}} \\ g_i(x,t) = \sum_{\{x_i,\{t_i\}\}} \delta(x-x_i)\sum_{t_i}\mathcal{H}(t-t_i)Q_i(x)\,e^{-\frac{t-t_i}{\tau_i(x)}} \end{cases} \quad (2)$$

where g_e and g_i are linear densities of conductances. Each synapse, indexed by s, has a position x_s and a set of presynaptic events $\{t_s\}$, hence the iteration over $\{x_s,\{t_s\}\}$ for the sum over synapses for each synaptic type. $\mathcal{H}$ is the Heaviside step function. The presynaptic events $\{t_s\}$ are generated by point processes at fixed frequencies ν_s with a given degree of synchrony, see details in the previous section V.3.

The model distinguishes two domains : a proximal domain with the upper index p and a distal domain with the upper index d (see Figure 1). Then the space-dependent quantities (presynaptic frequencies, synaptic quantal and synaptic decay time constant) can be written as :

$$\begin{cases} \nu_e(x) = \nu_e^P + (\nu_e^d - \nu_e^p)\mathcal{H}(x-l_p) \\ \nu_i(x) = \nu_i^P + (\nu_i^d - \nu_i^p)\mathcal{H}(x-l_p) \\ Q_e(x) = Q_e^P + (Q_e^d - Q_e^p)\mathcal{H}(x-l_p) \\ Q_i(x) = Q_i^P + (Q_i^d - Q_i^p)\mathcal{H}(x-l_p) \\ \tau_e(x) = \tau_e^P + (\tau_e^d - \tau_e^p)\mathcal{H}(x-l_p) \\ \tau_i(x) = \tau_i^P + (\tau_i^d - \tau_i^p)\mathcal{H}(x-l_p) \end{cases} \quad (3)$$

The continuity of the membrane potential and of the current at the boundaries between the proximal and distal part imply:

$$\begin{cases} v(l_p^-,t) = v(l_p^+,t) \\ \frac{1}{r_i}\frac{\partial v}{\partial x}_{l_p^-} = \frac{1}{r_i}\frac{\partial v}{\partial x}_{l_p^+} \end{cases} \quad (4)$$

where the limit with upper index $\pm$ indicate the limit taken from the left or the right respectively.

At the soma, $(x=0)$, we have a lumped impedance compartment. It has leaky RC circuit properties and also receives synaptic inhibition, the somatic membrane potential therefore follows :

$$\begin{cases} C_M\frac{dV}{dt} + \frac{V-E_L}{R_M} + G_I(t)\,(V-E_i) + I(t) = 0 \\ G_i(t) = \sum_{N_i}\sum_{\{t_i\}} Q_i^p\, e^{-\frac{-(t-t_i)}{\tau_i^p}}\,\mathcal{H}(t-t_i) \end{cases} \quad (5)$$

where $I(t)$ is the time-dependent input current from the soma into the dendrite. R_M and C_M are the RC properties of the lumped compartment (capital letters will indicate the somatic properties throughout the calculus). N_i is the number of somatic synapses, each of them generates a point process $\{t_i\}$ of inhibitory synaptic events. The properties of the somatic synapses $(\nu_i^d, Q_i^d, \tau_i^d)$ are equivalent to the proximal ones.

This equation with the membrane potential continuity will determine the boundary condition at the soma (x=0). We identify $V(t) = v(0,t)$, then $I(t)$ is the current input into the dendritic tree at $x=0$ so it verifies:

$$\frac{\partial v}{\partial x}_{|x=0} = -r_i\, I(t) \quad (6)$$

So:

$$\frac{\partial v}{\partial x}_{|x=0} = r_i\left(C_M\frac{\partial v}{\partial t}_{|x=0} + \frac{v(0,t)-E_L}{R_m} + G_I(t)\,(v(0,t)-E_i)\right) \quad (7)$$

Finally, the last boundary condition is that all branches terminate with an infinite resistance that impede current flow (sealed-end boundary conditions):

$$\frac{\partial v}{\partial x}_{x=l} = 0 \quad (8)$$

Together with the biased Poisson process for event generation (see previous section V.3), the final set of equations that describes the model, is therefore:

$$\begin{cases} \frac{1}{r_i}\frac{\partial^2 v}{\partial x^2} = c_m\frac{\partial v}{\partial t} + \frac{v-E_L}{r_m} - i_{syn}(v,x,t) \\ \frac{\partial v}{\partial x}_{|x=0} = r_i\left(C_M\frac{\partial v}{\partial t}_{|x=0} + \right. \\ \qquad \left. \frac{v(0,t)-E_L}{R_m} + G_I(t)\left(v(0,t)-E_i\right)\right) \\ v(l_p^-,t) = v(l_p^+,t) \\ \frac{\partial v}{\partial x}_{l_p^-} = \frac{\partial v}{\partial x}_{l_p^+} \\ \frac{\partial v}{\partial x}_{x=l} = 0 \end{cases} \quad (9)$$

V.5 Numerical implementation

The full model has been implemented numerically using the `NEURON` software. The branched morhology was created and passive cable properties were introduced. The spatial discretization was `nseg=30` segments per branch. On each segment, one excitatory and one inhibitory synapse were created, the shot-noise frequency was then scaled according to the segment area and the synaptic density to account for the number of synapses on this segment (using the properties of the Poisson process, N synapses at frequency ν is a synapse at frequency $N\nu$). Custom event generation was implemented to introduce correlations (instead of classical `NetStim`) and fed `NetCon` objects attached to each synapses (`ExpSyn` synapses).

V.6 Strategy for the analytical derivation

We present here a derivation that provides an analytical approximation for the properties of the fluctuations of the membrane potential at the soma for our model. Summing up its properties, we get: 1) a morphology with a lumped somatic compartement and a dendritic tree of symmetric branching following Rall's rule 2) conductance-based synapses 3) independent excitatory and inhibitory shotnoise input spread all over the morphology 4) assymetric properties between a proximal part and a distal part and 5) a certain degree of synchrony in the pre-synaptic spikes.

The properties of the membrane potential fluctuations at the soma correspond to three stationary statistical properties of the fluctuations: their mean μ_V, their standard deviation σ_V and their *global* autocorrelation time τ_V. Following Zerlaut et al. (2016), we emphasize that the *global* autocorrelation time is a partial description of the autocorrelation function (as the autocorrelation function is not exponential) but it constitues the first order description of the temporal dynamics of the fluctuations.

A commonly adopted strategy in the *fluctuation-driven* regime to obtain statistical properties is to use stochastic calculus after having performed the *diffusion approximation*, i.e. approximating the synaptic conductance time course by a stochastic process, see e.g. (Tuckwell et al., 2002)). This approach is nonetheless not easily generalizable to conductance input in an extended structure and render the inclusion of assymetric properties (proximal vs distal) complicated. We rather propose here an approach that combines simplifying assumptions and analytical results from shotnoise theory, it constitues an extension of the approach proposed in Kuhn et al. (2004).

For each set of synaptic stimulation $\{\nu_p^e, \nu_i^p, \nu_e^d, \nu_i^d, s\}$, the derivation corresponds to the following steps:

- We transform the dendritic structure to its equivalent cylinder. The reduction to the equivalent cylinder is "activity-dependent" and captures the changes in membrane properties that results from the mean synaptic conductance levels.
- We derive a mean membrane potential $\mu_V(x)$ corresponding to the stationary response to constant densities of conductances given by the means of the synaptic stimulation. We use this space-dependent membrane potential $\mu_V(x)$ to fix the driving force all along the membrane for all synapses. The relation between synaptic events and the membrane potential now becomes linear.
- We derive a new cable equation that describes the variations of the membrane potential around this $\mu_V(x)$ solution.
- We calculate the effect of one synaptic event on a branch $b, b \in [1, B]$ at a distance x. We calculate the post-synaptic membrane potential event $\mathrm{PSP}_b(x,t)$ at the soma resulting from b synchronous synaptic events occuring at the distance x from the soma. We approximate the effect of only one event by rescaling the response by the number of input $\mathrm{PSP}_b(x,t)/b$.
- We use shotnoise theory to compute the power spectrum density of the membrane potential fluctuations resulting from all excitatory and inhibitory synaptic events (including the synchrony between events).

The full derivation has been conducted with the help of the python modulus for symbolic computation: `sympy` (deriving homogenous solutions is relatively simple but computing coefficients with the boudaries conditions give rise to complex expressions because of the number of parameters). The resulting expression were then exported to `numpy` functions for numerical evaluation. The `ipython` notebook that presents the full derivation is available on the following link.

V.7 Reduction to an equivalent cylinder

The key of the derivation relies on having the possibility to reduce the complex morphology to an equivalent cylinder (Rall, 1962). We adapted this procedure to capture the change in integrative properties of the membrane that results from the mean synaptic bombardment during active cortical states, reviewed in Destexhe et al. (2003).

For a set of synaptic stimulation $\{\nu_p^e, \nu_i^p, \nu_e^d, \nu_i^d, s\}$, let's introduce the following stationary densities of conductances:

$$\begin{cases} g_{e0}^p = \pi\, d\, \mathcal{D}_e\, \nu_e^p\, \tau_e^p\, Q_e^p \quad ; \quad g_{i0}^p = \pi\, d\, \mathcal{D}_i\, \nu_i^p\, \tau_i^p\, Q_i^p \\ g_{e0}^d = \pi\, d\, \mathcal{D}_e\, \nu_e^d\, \tau_e^d\, Q_e^d \quad ; \quad g_{i0}^d = \pi\, d\, \mathcal{D}_i\, \nu_i^d\, \tau_i^d\, Q_i^d \end{cases} \quad (10)$$

where $\mathcal{D}_e$ and $\mathcal{D}_i$ are the excitatory and inhibitory synaptic densities (see Figure 1B).

We introduce two activity-dependent electrotonic constants relative to the proximal and distal part respectively:

$$\lambda^p = \sqrt{\frac{r_m}{r_i(1+r_m g_{e0}^p + r_m g_{i0}^p)}} \quad \lambda^d = \sqrt{\frac{r_m}{r_i(1+r_m g_{e0}^d + r_m g_{i0}^d)}} \quad (11)$$

For a dendritic tree of total length l, whose proximal part ends at l_p and with B evenly spaced generations of branches, we define the space-dependent electrotonic constant:

$$\lambda(x) = \left(\lambda^p + \mathcal{H}(x-l_p)(\lambda^d - \lambda^p)\right) 2^{-\frac{1}{3}\lfloor \frac{B\,x}{l} \rfloor} \tag{12}$$

where $\lfloor . \rfloor$ is the floor function. Note that $\lambda(x)$ is constant on a given generation, but it decreases from generation to generation because of the decreasing diameter along the dendritic tree. It also depends on the synaptic activity and therefore has a discontinuity at $x = l_p$.

Following Rall (1962), we now define a dimensionless length X:

$$X(x) = \int_0^x \frac{dx}{\lambda(x)} \tag{13}$$

We define $L = X(l)$ and $L_p = X(l_p)$, the total length and proximal part length respectively (capital letters design rescaled quantities).

V.8 Mean membrane potential

We derive the mean membrane potential $\mu_V(x)$ corresponding to the stationary response to constant densities of conductances given by the means of the synaptic stimulation. We obtain the stationary equations by removing temporal derivatives in Equation, the set of equation governing this mean membrane potential in all branches is therefore:

$$\begin{cases} \frac{1}{r_i}\frac{\partial^2 \mu_v}{\partial x^2} = \frac{\mu_v(x) - E_L}{r_m} \\ \qquad - g^p_{e0}\left(\mu_v(x) - E_e\right) - g^p_{0i}\left(\mu_v(x) - E_i\right) \quad \forall x \in [0, l_p] \\ \frac{1}{r_i}\frac{\partial^2 \mu_v}{\partial x^2} = \frac{\mu_v(x) - E_L}{r_m} \\ \qquad - g^d_{e0}\left(\mu_v(x) - E_e\right) - g^d_{0i}\left(\mu_v(x) - E_i\right) \quad \forall x \in [l_p, l] \\ \frac{\partial \mu_v}{\partial x}_{|x=0} = r_i\left(\frac{\mu_v(0) - E_L}{R_m} + G^S_{i0}\left(\mu_v(0) - E_i\right)\right) \\ \mu_v(l_p^-, t) = \mu_v(l_p^+, t) \\ \frac{\partial \mu_v}{\partial x}_{l_p^-} = \frac{\partial \mu_v}{\partial x}_{l_p^+} \\ \frac{\partial \mu_v}{\partial x}_{x=l} = 0 \end{cases} \tag{14}$$

Because the reduction to the equivalent cylinder conserves the membrane area and the previous equation only depends on density of currents, the equation governing $\mu_v(x)$ in all branches can be transformed into an equation on an equivalent cylinder of length L. We rescale x by $\lambda(x)$ (see Equation 13) and we obtain the equation verified by $\mu_V(X)$:

$$\begin{cases} \frac{\partial^2 \mu_v}{\partial X^2} = \mu_v(X) - v_0^p \quad \forall X \in [0, L_p] \\ \frac{\partial^2 \mu_v}{\partial X^2} = \mu_v(X) - v_0^d \quad \forall X \in [L_p, L] \\ \frac{\partial \mu_v}{\partial X}|_{X=0} = \gamma^p\left(\mu_v(0) - V_0\right) \\ \mu_v(L_p^-) = \mu_v(L_p^+) \\ \frac{\partial \mu_v}{\partial X}_{L_p^-} = \frac{\lambda^p}{\lambda^d}\frac{\partial \mu_v}{\partial X}_{L_p^+} \\ \frac{\partial \mu_v}{\partial X}_{X=L} = 0 \end{cases} \tag{15}$$

where:

$$\begin{aligned} v_0^p &= \frac{E_L + r_m g^p_{e0} E_e + r_m g^p_{i0} E_i}{1 + r_m g^p_{e0} + r_m g^p_{i0}} \\ v_0^d &= \frac{E_L + r_m g^d_{e0} E_e + r_m g^d_{i0} E_i}{1 + r_m g^d_{e0} + r_m g^d_{i0}} \\ \gamma^p &= \frac{r_i \lambda^p \left(1 + G^0_i R_m\right)}{R_m} \\ V_0 &= \frac{E_L + G^0_i R_m E_i}{1 + + G^0_i R_m} \end{aligned} \tag{16}$$

The solution for this equation is:

$$\mu_v(X) = \begin{cases} v_0^p + A\cosh(X) + (v_0^p - V_0 + A)\sinh(X), \\ \qquad \forall X \in [0, L_p] \\ v_0^d + B\cosh(X - L), \quad \forall X \in [L_p, L] \end{cases} \tag{17}$$

with A and B explicited in the supplementary material. The accuracy of this expression can be seen on Figure 3.

V.9 Membane potential response to a synaptic event

We now look for the response to $n_{src} = \lfloor \frac{B\,x_{src}}{l} \rfloor$ synaptic events at position x_{src} on all branches of the generation of $x_s rc$, those events have a conductance $g(t)/n_{src}$ and reversal potential E_{rev}. We make the hypothesis that the initial condition correspond to the stationary mean membrane potential $\mu_V(x)$. This potential will also be used to fix the driving force at the synapse to $\mu_v(x_{src}) - E_{rev}$, this linearizes the equation and will allow an analytical treatment. To derive the equation for the response around the mean $\mu_v(x)$, we rewrite Equation 9 with $v(x,t) = \delta v(x,t) + \mu_v(x)$, we obtain the equation for $\delta v(x,t)$:

$$\begin{cases} \frac{1}{r_i}\frac{\partial^2 \delta v}{\partial x^2} = c_m\frac{\partial \delta v}{\partial t} + \frac{\delta v}{r_m}(1 + r_m\, g^p_{e0} + r_m\, g^p_{i0}) \\ \qquad - \delta(x - x_{src})\left(\mu_v(x_{src}) - E_{rev}\right)\frac{g(t)}{n_{src}}, \quad \forall x \in [0, l_p] \\ \frac{1}{r_i}\frac{\partial^2 \delta v}{\partial x^2} = c_m\frac{\partial \delta v}{\partial t} + \frac{\delta v}{r_m}(1 + r_m\, g^d_{e0} + r_m\, g^d_{i0}) \\ \qquad - \delta(x - x_{src})\left(\mu_v(x_{src}) - E_{rev}\right)\frac{g(t)}{n_{src}}, \quad \forall x \in [l_p, l] \\ \frac{1}{r_i}\frac{\partial \delta v}{\partial x}_{|x=0} = C_M\frac{\partial \delta v}{\partial t}_{|x=0} + \frac{\delta v(0,t)}{R_m}(1 + R_m G^S_{i0}) \\ \delta v(l_p^-, t) = \delta v(l_p^+, t) \\ \frac{\partial \delta v}{\partial x}_{l_p^-} = \frac{\partial \delta v}{\partial x}_{l_p^+} \\ \frac{\partial \delta v}{\partial x}_{x=l} = 0 \end{cases} \tag{18}$$

Because this synaptic event is concomitant in all branches at distance x_{src}, we can use again the reduction to the equivalent cylinder (note that the event has now a weight multiplied by n_{src} so that its conductance becomes $g(t)$), we obtain:

$$\begin{cases} \frac{\partial^2 \delta v}{\partial X^2} = \left(\tau_m^p + (\tau_m^d - \tau_m^p)\mathcal{H}(X - L_p)\right)\frac{\partial \delta v}{\partial t} + \delta v \\ \qquad - \left(\mu_v(X_{src}) - E_{rev}\right)\delta(X - X_{src})\times \\ \qquad\qquad \frac{g(t)}{c_m}\left(\frac{\tau_m^p}{\lambda^p} + (\frac{\tau_m^d}{\lambda^d} - \frac{\tau_m^p}{\lambda^p})\mathcal{H}(X_{src} - L_p)\right) \\ \frac{\partial \delta v}{\partial X}_{|X=0} = \gamma^p\left(\tau_m^S \frac{\partial \delta v}{\partial t}_{|X=0} + \delta v(0,t)\right) \\ \delta v(L_p^-, t) = \delta v(L_p^+, t) \\ \frac{\partial \delta v}{\partial X}_{L_p^-} = \frac{\lambda^p}{\lambda^d}\frac{\partial \delta v}{\partial X}_{L_p^+} \\ \frac{\partial \delta v}{\partial X}_{X=L} = 0 \end{cases} \quad (19)$$

where we have introduced the following time constants:

$$\begin{aligned} \tau_m^D &= \frac{r_m\, c_m}{1 + r_m\, g_{e0}^d + r_m\, g_{i0}^d} \\ \tau_m^P &= \frac{r_m\, c_m}{1 + r_m\, g_{e0}^p + r_m\, g_{i0}^p} \\ \tau_m^S &= \frac{R_m\, C_m}{1 + R_m\, G_{i0}^S} \end{aligned} \quad (20)$$

Now used distribution theory (see Appel (2008) for a comprehensive textbook) to translate the synaptic input into boundary conditions at X_{src}, physically this corresponds to: 1) the continuity of the membrane potential and 2) the discontinuity of the current resulting from the synaptic input.

$$\begin{cases} \delta v(X_{src}^-, f) = \delta v(X_{src}^+, f) \\ \frac{\partial \delta v}{\partial X}_{X_{src}^+} - \frac{\partial \delta v}{\partial X}_{X_{src}^-} = -\left(\mu_v(X_{src}) - E_{rev}\right)\times \\ \qquad \left(\frac{\tau_m^p}{\lambda^p} + (\frac{\tau_m^d}{\lambda^d} - \frac{\tau_m^p}{\lambda^p})\mathcal{H}(X_{src} - L_p)\right)\frac{g(t)}{c_m} \end{cases} \quad (21)$$

We will solve Equation 19 by using Fourier analysis. We take the following convention for the Fourier transform:

$$\hat{F}(f) = \int_{\mathbb{R}} F(t)\, e^{-2i\pi f t}\, dt \quad (22)$$

We Fourier transform the set of Equations 19, we obtain:

$$\begin{cases} \frac{\partial^2 \hat{\delta v}}{\partial X^2} = \left(\alpha_f^p + (\alpha_f^d - \alpha_f^p)\mathcal{H}(X - L_p)\right)^2 \hat{\delta v} \\ \frac{\partial \hat{\delta v}}{\partial X}_{|X=0} = \gamma_f^p\, \hat{\delta v}(0, f) \\ \hat{\delta v}(X_{src}^-, f) = \hat{\delta v}(X_{src}^+, f) \\ \frac{\partial \hat{\delta v}}{\partial X}_{X_{src}^-} = \frac{\partial \hat{\delta v}}{\partial X}_{X_{src}^+} - \left(\mu_v(X_{src}) - E_{rev}\right)\times \\ \qquad\qquad \left(r_f^p + (r_f^d - r_f^p)\mathcal{H}(X_{src} - L_p)\right)\hat{g(f)} \\ \hat{\delta v}(L_p^-, f) = \hat{\delta v}(L_p^+, f) \\ \frac{\partial \hat{\delta v}}{\partial X}_{L_p^-} = \frac{\lambda^p}{\lambda^d}\frac{\partial \hat{\delta v}}{\partial X}_{L_p^+} \\ \frac{\partial \hat{\delta v}}{\partial X}_{X=L} = 0 \end{cases} \quad (23)$$

where

$$\begin{aligned} \alpha_f^p &= \sqrt{1 + 2i\pi f \tau_m^p} \qquad r_f^p = \frac{\tau_m^p}{c_m\, \lambda^p} \\ \alpha_f^d &= \sqrt{1 + 2i\pi f \tau_m^d} \qquad r_f^d = \frac{\tau_m^d}{c_m\, \lambda^d} \\ \gamma_f^p &= \gamma^p\,(1 + 2i\pi f \tau_m^S) \end{aligned} \quad (24)$$

This equation is solved in the supplementary material. We will use the solution at the soma, it can be written:

$$\hat{\delta v}(X = 0, X_{src}, f) = K_f(X_{src})\left(\mu_v(X_{src}) - E_{rev}\right)\hat{g(f)} \quad (25)$$

V.10 Deriving the fluctuations properties

From shotnoise theory (Daley and Vere-Jones, 2007) (see also El Boustani et al. (2009) for an application similar to ours), we can obtain the power spectral density of the V_m fluctuations $P_V(f)$ as a response to the stimulation Equation *eq:fluct-eq*:

From point process theory, this can be seen as two nested point processes. The first point process follows a Poisson process which determines the cluster positions and the second one determines randomly the position of kz1 points within each cluster according to an arbitrary density probability function. The correspondance between both representations is straightforward and the power spectrum density can be computed analytically with the Neyman- Scott equation [23,24,51]

$$\begin{aligned} P_V(f) &= \sum_{syn} \nu_{syn}\, \|\hat{\mathrm{PSP}}(f)\|^2 \\ &= 2\nu_{in}\, \frac{Q_I^2\, \tau_S^2/\mu_G^2}{(1 + 4\pi^2 f^2 \tau_S^2)(1 + 4\pi^2 f^2 \tau_m^2)} \end{aligned} \quad (26)$$

$$\tau_V = \frac{1}{2}\left(\frac{\int_{\mathbb{R}} P_V(f)\, df}{P_V(0)}\right)^{-1} \quad (27)$$

$$\sigma_V^2 = \int_{\mathbb{R}} P_V(f)\, df \quad (28)$$

V.11 From fluctuation properties to spiking probability

Focus of a previous communication, see Zerlaut et al. (2016).

V.12 Experimental preparation and electrophysiological recordings

Experimental methods were identical to those presented in Zerlaut et al. (2016). Very briefly, we performed intracellular patch-clamp recordings using the perforated patch technique on layer V pyramidal neurons of coronal slices of juvenile mice primary visual cortex. For the n=13 cells presented in this study, the access resistance R_S was *XX* MΩ ± *YY*, the leak current at -75mV was *XX* pA ± *YY*, cells had an input resistance R_m of *XX* MΩ ± *YY* and a membrane time constant at rest of *XX* ms ± *YY*.

V.13 Input impedance characterization

To determine the input impedance at the soma, we injected sinusoidal currents in the current-clamp mode of the amplifier (Multiclamp 700B, Molecular Devices), we recorded the membrane potential response to a current input of the form $I(t) = I\,\sin(2\pi\, f\, t)$, we varied the frequencies f and amplitudes $I over 40 episodes per cell. The frequency range scanned was [0.1, 500] Hz. For each cell, we determined manually the current amplitude I_0 that gave a $\sim$ 5mV amplitude in a current step protocol, from this value, the value of I was scaled exponentially between I_0 at 0.1 Hz and $50I_0$ at 500Hz. The reason for varying the current amplitude (and not only the oscillation

frequency) in those input impedance protocols is to anticipate for the low pass filtering of the membrane and insure that the membrane potential response at high frequencies is far above the electronic noise level ($\sim$ 0.1 mV).

After removing the first 3 periods of the oscillations (to avoid transient effects), we fitted the membrane potential response to the form:

$$V(t) = E_L + R\,I\,\sin(2\pi\,f\,t - \phi) \qquad (29)$$

where E_L, R and ϕ were fitted with a least-square minimization procedure. The frequency dependent values of R and ϕ give the modulus and phase shift of the input impedance presented in Figure 2A

V.14 Numerical tools

All numerical simulations of single cell dynamics have been performed with custom code written in the numerical library of `python`: `numpy` and optimized with the `numba` library. For the neuronal model, each point (a mean output frequency and its standard deviation across trials) corresponds to numerical simulations running with a time step dt=0.01ms, for a duration of 10s and repeated 4 times with different seeds (one simulation duration: $\sim$ 2s of real time on a Dell Optiplex 9020 desktop computer). Experimental protocols and online-analysis have been written in `Elphy2`. Plots and data analysis have been done thanks to the `SciPy` package.

V.15 Acknowledgments

Y.Z was supported by fellowships from the Initiative d'Excellence Paris-Saclay and the Fondation pour la Recherche Médicale (FDT 20150532751). Research funded by the CNRS, the ANR (Complex-V1 project) and the European Community (BrainScales FP7-269921 and the Human Brain Project FP7-604102). The authors declare no competing financial interests.

VI References

Appel W (2008) *Mathématiques pour la physique et les physiciens* H. et K. Editions.

Daley DJ, Vere-Jones D (2007) *An introduction to the theory of point processes: volume II: general theory and structure*, Vol. 2 Springer Science & Business Media.

Debanne D, Campanac E, Bialowas A, Carlier E, Alcaraz G (2011) Axon physiology. *Physiological reviews* 91:555–602.

Destexhe A, Rudolph M, Paré D (2003) The high-conductance state of neocortical neurons in vivo. *Nature reviews. Neuroscience* 4:739–751.

El Boustani S, Marre O, Béhuret S, Baudot P, Yger P, Bal T, Destexhe A, Frégnac Y (2009) Network-state modulation of power-law frequency-scaling in visual cortical neurons. *PLoS computational biology* 5:e1000519.

Kuhn A, Aertsen A, Rotter S (2004) Neuronal integration of synaptic input in the fluctuation-driven regime. *The Journal of neuroscience : the official journal of the Society for Neuroscience* 24:2345–56.

Rall W (1962) Electrophysiology of a dendritic neuron model. *Biophysical journal* 2:145.

Stuart GJ, Spruston N (2015) Dendritic integration: 60 years of progress. *Nature Neuroscience* 18:1713–1721.

Tuckwell HC, Wan FYM, Rospars JP (2002) A spatial stochastic neuronal model with Ornstein–Uhlenbeck input current. *Biological cybernetics* 86:137–145.

Zerlaut Y, Telenczuk B, Deleuze C, Bal T, Ouanounou G, Destexhe A (2016) Heterogeneous firing response of mice layer V pyramidal neurons in the fluctuation-driven regime. *in revision* .